Pergamon

0042-6989(94)00193-6

Vision Res. Vol. 35, No. 7, pp. 907–914, 1995

0042-6989/95 $9.50 + 0.00

Spatiotemporal Characterization of a Fourier and Non-Fourier Motion System

ANDREI GOREA*

Received 19 July 1993; in revised form 10 March 1994; in final form 10 August 1994

Direct-phi perception elicited by a reverse-phi (i.e. reversed-polarity) stimulus may well be accounted for, if the front-end filters of a classical Reichardt unit are full-wave rectifiers. It is shown that reverse-phi perception is progressively replaced by direct-phi perception when either the spatial or the temporal modulation of the reversed-polarity stimuli are decreased. Reverse-phi perception is very weak or absent for spatial and temporal frequencies $\leqslant 1$ c/deg and $\leqslant 3.75$ Hz, respectively, indicating that the sensitivity of a linear mechanism is weak or null within this frequency range. By pitting against each other reverse- and direct-phi stimuli, the relative sensitivities of the putative motion mechanisms with linear (Fourier) and full-wave rectified (non-Fourier) front-end filters were assessed for a large range of spatial and temporal frequencies. Absolute sensitivities of the two mechanisms were estimated on the assumption that they contribute through probability summation to the overall spatiotemporal sensitivity surface described by Kelly [(1979) *Journal of the Optical Society of America, 69,* 1340–1349]. In conjunction with related evidence it is suggested that the Fourier/non-Fourier distinction may be generalized in terms of a *specific/unspecific* dichotomy in motion processing.

Motion processing Direct-phi Reverse-phi Specific motion systems Unspecific motion systems

INTRODUCTION

The latest dichotomy put forth to account for human motion perception refers to Fourier (or first-order) and non-Fourier (or second-order) motion systems (Chubb & Sperling, 1987, 1988a, b, 1989a b; Wilson, Ferrera & Yo, 1992). The parallel activation of Reichardt-type detectors (or of equivalent spatiotemporal energy detectors; Adelson & Bergen, 1985; Van Santen & Sperling, 1984, 1985) whose front-end spatiotemporal receptive fields behave either as (quasi-)linear filters (Fourier system) or as full-wave rectifiers (non-Fourier system), appears to account for most (if not all) motion perception phenomena observed with luminance-modulated stimuli (see Sperling, 1989 for a review). Among these, reverse-phi perception (Anstis, 1980) and its disappearance under some experimental conditions (such as low-passed stimuli, high contrasts, etc., Chubb & Sperling, 1988a, 1989b) are most readily accounted for if one assumes that the two motion systems display distinct spatiotemporal characteristics.

Typically, a "reverse-phi" stimulus, namely a stimulus whose contrast is reversed at each animation step, yields a perceived direction opposite to its physical displacement. The phenomenon is straightforwardly accounted for in terms of the spatiotemporal Fourier spectrum of the stimulus as obtained after convolution with a linear spatiotemporal filter; most of its energy lies indeed along the direction opposite to the physical displacement. The reverse picture is obtained (i.e. most of the spatiotemporal energy lies along the physical direction) if the spatiotemporal filter behaves as a full-wave rectifier (Anstis & Mather, 1985; Chubb & Sperling, 1989b; Sperling, 1989). Thus, depending on which of the two motion systems is more strongly activated, a reverse-phi stimulus will yield opposite perceived directions. In contrast, processing a regular drifting stimulus by either of the two mechanisms will always yield a perceived direction coinciding with its physical displacement. In an attempt to specify the spatiotemporal characteristics of the two motion mechanisms, the present study takes advantage of the perceptually conflicting situations elicited by the simultaneous presentation of a reverse- and of a direct-phi stimulus under a variety of spatiotemporal conditions.

RATIONALE AND STIMULUS CONFIGURATIONS

The present experiments were not meant to assess the existence of two motion systems. Rather, they were built on the *premise* that they *do* exist. The rationale exposed here would be meaningless otherwise. Moreover, these experiments were not intended to provide an independent characterisation of these putative mechanisms. Rather, they bear on their *relative* spatiotemporal sensitivities, S_I/S_{II} (with I and II referring to first- (Fourier) and second-order (non-Fourier) systems, respectively).

*Laboratoire de Psychologie Expérimentale, Université René Descartes and C.N.R.S., 28 rue Serpente, 75006 Paris, France.

S_I and S_{II} can, nonetheless, be specified if one assumes that the two mechanisms are independent and that the overall visual sensitivity is given by the probabilistic sum of their sensitivities (see below). The estimation of the S_I/S_{II} ratios is based on a simplified account of motion processing by Reichardt-type detectors. These simplifications are as follows.

For any given speed, the underlying Reichardt unit is *optimal*; this means that the temporal shift between the outputs of the two spatial front-end filters to the cross-correlation stage *strictly matches* the delay with which the stimulus activates these front-end filters. As a consequence, the cross-correlation in the Reichardt subunit tuned to the actual stimulus direction degenerates into a squaring operation. Squaring and time-averaging (e.g. Van Santen & Sperling, 1984, 1985) these responses for the Fourier and non-Fourier systems will come up with *identical* values (i.e. energies) which will cancel out when computing the S_I/S_{II} ratio. Thus, except for assuming their linear or full-wave rectified response, front-end filtering (mono- or biphasic) can be ignored when computing the S_I/S_{II} ratios for Reichardt subunits optimally tuned to a given velocity. Accordingly, the response of the Reichardt detector is given *directly* by the *covariance product*, in the stimulus space, of a pair of events displaced in space and time. This simplification was used in a number of recent studies (Werkhoven, Snippe & Koenderink, 1990; Werkhoven, Chubb & Sperling, 1993; Chubb, McGowan, Sperling & Werkhoven, personal communication; Gorea, Papathomas & Kovacs, 1993a, b).

The covariance product in the stimulus space is not, however, a fair indicator of the motion response if one takes into account the inherent opponent nature of the Reichardt unit (Adelson & Bergen, 1985). Its overall response is given by subtracting from the response of the subunit tuned to the direction of the stimulus the response of the opponent subunit. For an optimal Reichardt detector (in the sense described above), the opponent subunit displays a temporal shift of opposite sign so that the total delay to its cross-correlation stage is twice the stimulus delay. In this case, the cross-correlation product does not reduce to a squaring operation. The outputs of the cross-correlation plus time averaging stage will be different in a linear and in a full-wave rectification system *for any non-monophasic front-end filtering*. It follows that, in a S_I/S_{II} ratio computation, the coefficients of the Fourier (μ) and non-Fourier (γ) systems no longer cancel out. The covariance product in the stimulus space must then be weighted by these coefficients.

A final simplification used in the estimation of the S_I/S_{II} ratios concerns the space-time separability. It has been well established since Robson (1966) that the temporal impulse response of the visual system (as it was assessed psychophysically) is spatial frequency dependent. It smoothly changes from a biphasic to a monophasic profile when spatial frequency increases. The computation of the μ and γ coefficients was simplified by using a purely biphasic (i.e. zero d.c.) temporal response for spatial frequencies equal to or below 2 c/deg and a purely monophasic impulse response for all the remaining frequencies.* This approximation seems reasonable in view of the psychophysical data (Robson, 1966; Kelly, 1969; Gorea & Tyler, 1986).

Under the simplified covariance metric adopted here, the responses, R_I and R_{II} of the Fourier and non-Fourier units are given by

$$R_I = \mu \times D \times S_I \times C_{i,j} \times C_{i+1,j+1} \quad (1)$$

$$R_{II} = \gamma \times D \times S_{II} \times |C_{i,j} \times C_{i+1,j+1}|, \quad (2)$$

where D is a sign parameter arbitrarily set to $+$ or -1 depending on whether the physical displacement is to the right or to the left and C is the contrast of the drifting stimulus at position i and time j and when displaced in space–time at $i+1, j+1$. If the absolute value of C does not change across space–time, then equations (1) and (2) reduce to

$$R_I = \mu \times D \times S_I \times \pm C^2 \quad (3)$$

$$R_{II} = \gamma \times D \times S_{II} \times C^2. \quad (4)$$

One would then like to build a stimulus where R_I and R_{II} cancel out so that S_I and S_{II} can be expressed as a function of each other. Figure 1 displays a space–time (x–t) diagram (the y dimension is omitted) of the two stimulus configurations used in the present study.

The left side of Fig. 1A displays stimulus configuration #1, where the direct- and reverse-phi stimuli are drifting along the same physical direction (i.e. rightward; $D = +1$). The digits within each square of this space–time display refer to specific and independent contrasts. The Fourier mechanism will "see" this configuration as displayed. The non-Fourier mechanism, assumed to behave as a full-wave rectifier, will "see" configuration #1 as it is displayed on the right side of Fig. 1A, i.e. negative polarities will be processed as positive polarities. Thus, since the non-Fourier

*The analytical form of the monophasic and biphasic temporal impulse responses $h(t)$ was taken from Watson (1982). The front-end temporal response of each subunit of the Reichardt detector, $H_{right}(t) = H_{left}(t)$, was computed as the convolution of the stimulus $f(t)$ with $h(t)$. $H(t)$ was full-wave rectified for the non-Fourier system. The output $R(t)$ of the cross-correlation stage was then obtained as $R_{right}(t) = H(t) \times H(t) = H^2(t)$, for the preferred direction, and as $R_{left}(t) = H(t) \times H(t + 2\Delta t)$, for the opposite direction (with Δt being the *optimal* time shift matching the stimulus delay). $R_{right}(t)$ and $R_{left}(t)$ were integrated over time and then subtracted to obtain the final response R_I and R_{II} (for the Fourier and non-Fourier systems, respectively). For a monophasic $h(t)$, R_I and R_{II} are strictly identical and cancel out when estimating the sensitivity ratio of the two systems. For a biphasic $h(t)$, however, the opponent response $R_{left}(t)$ will be different in the two systems. Their response ratio needs then to be estimated computationally.

Note that $R_{left}(t)$ depends on the speed of the stimulus, i.e. on Δt: when the speed decreases, Δt increases and the value of the cross-correlation product $H(t) \times H(t + 2\Delta t)$ decreases. So it happens that for temporal frequencies below about 7 Hz the time integral of this product is very close to 0. Thus, below this limit the overall responses R_I and R_{II} will be practically equal even for biphasic impulse responses.

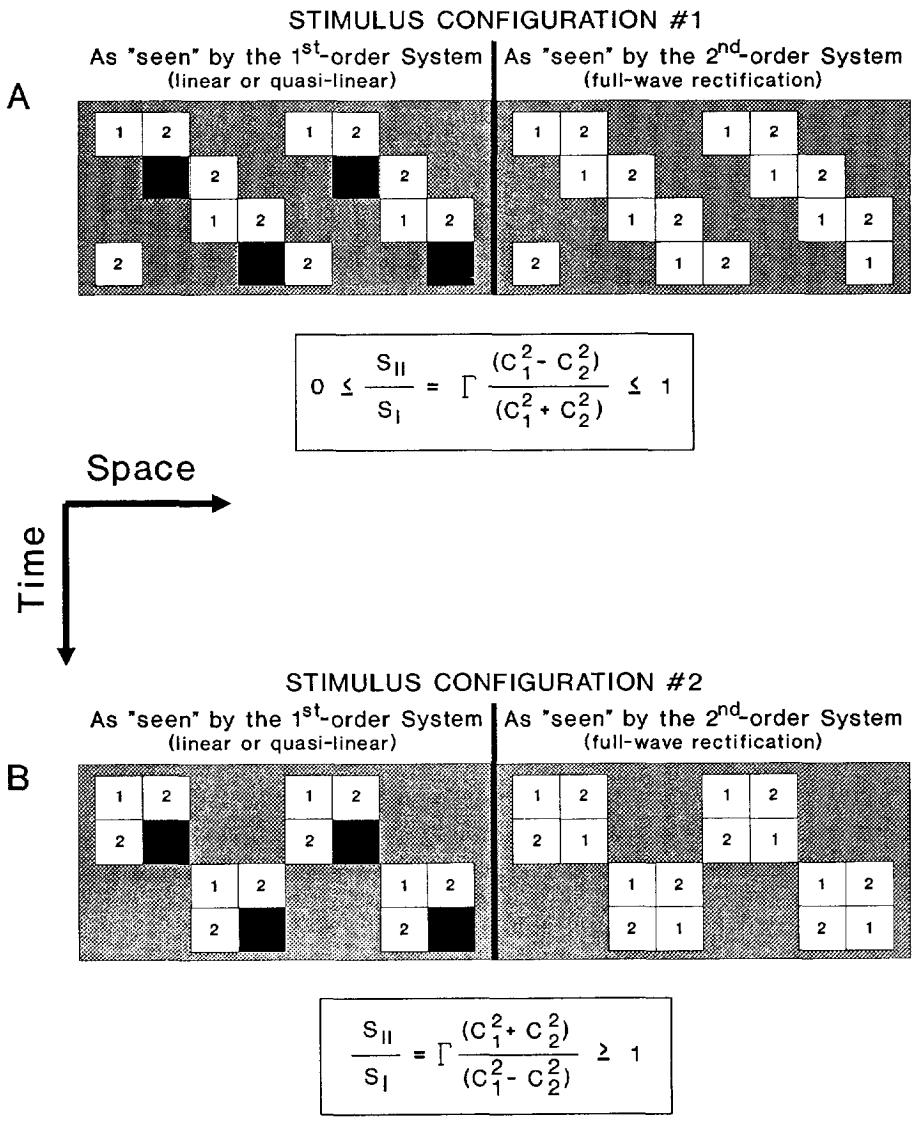

FIGURE 1. Space–time representation of the two stimulus configurations used in the present experiments. Each row represents one image frame. In Configuration #1 (A, left) direct- and reverse-phi stimuli are combined so as to yield the same *physical* direction (to the right). In Configuration #2 (B, left) the two components yield opposite physical directions. The contrasts of the two components (indexed "1" and "2" for the reverse- and direct-phi components, respectively) can be manipulated independently. White and dark squares stand for luminances above and below the background luminance (grey). The Fourier system "sees" the stimuli as actually displayed (left panels). The non-Fourier system is supposed to perform a full-wave rectification and "sees" the stimuli as shown in the right-hand panels. The sensitivity ratios as computed in this study are given by the equations below each panel with *S*, sensitivity; *D*, direction; *C*, contrast and Γ, the correction factor explained in the text. See text for more details.

mechanism will signal the same direction for the direct- and reverse-phi components of this configuration (i.e. their physical direction), a balanced left–right perception will be achieved only when the Fourier mechanism will provide a sufficiently strong output in the direction opposite to the physical displacement. When this is not the case, i.e. under spatiotemporal conditions where the reverse-phi phenomenon is *not* observed or is too weak, manipulating the relative contrasts (1 and 2) of the stimuli will never yield a reversal of the perceived direction. Configuration #2 (left side of Fig. 1B) was designed to be used under these particular conditions. Here again, the left side of Fig. 1B displays configuration #2 as actually presented and as "seen" by the Fourier system. The right side of Fig. 1B displays this same configuration as seen by the non-Fourier system, i.e. full-wave rectified.

The purpose of the experiment is to assess the contrasts of the reverse-phi (C_1) and of the direct-phi (C_2) components so that observers cannot reliably assess a particular drift direction. It is assumed that under this specific condition the overall response of the two mechanisms is null for the two stimulus configurations:

Configuration # 1

$$\gamma \times S_{II} \times C_1^2 - \mu \times S_I \times C_1^2 + \gamma \times S_{II} \times C_2^2 + \mu \times S_I \times C_2^2 = 0 \quad (5)$$

wherefrom,

$$S_{II}/S_I = \Gamma \times (C_1^2 - C_2^2)/(C_1^2 + C_2^2) \geq 0. \quad (6)$$

Configuration #2

$$-\gamma \times S_{II} \times C_1^2 + \mu \times S_I \times C_1^2 + \gamma \times S_{II} \times C_2^2 + \mu \times S_I \times C_2^2 = 0 \quad (7)$$

wherefrom,

$$S_{II}/S_I = \Gamma \times (C_1^2 + C_2^2)/(C_1^2 - C_2^2) \geq 0, \quad (8)$$

where $\Gamma = \gamma/\mu$. The simulations described in the footnote on p. 908 produced a Γ equal to 1 for all spatial frequencies higher than 2 c/deg (yielding monophasic temporal impulse responses) and for all temporal frequencies lower than 7.5 Hz. The simulations produced a Γ of 0.64 and 0.38 for spatial frequencies lower than 2 c/deg and for temporal frequencies of 7.5 and 15 Hz, respectively.

Notice that equations (6) and (8) require that $C_1^2 \geq C_2^2$ (i.e. sensitivities cannot be negative). Also notice that equations (7) and (9) are satisfied, i.e. the overall directional percept is null, only if $S_I > S_{II}$ and if $S_{II} > S_I$, respectively. Finally notice that the directional parameter D (± 1) is used in accordance with the directions exemplified in Figs 1A and 1B.

METHODS

Stimuli

The stimuli were vertical square-wave yellow (CIE x, y coordinates 0.448, 0.475) gratings displayed on a SONY Trinitron monitor (GDM 1601/1950) driven by an Adage PG-90/10 graphic card under the control of a LEANORD-386 AT computer. The Adage card provides 8 bits modulation (256 grey levels) per gun. The stimuli were presented at a mean luminance of 20 cd/m^2 and subtended a 6.5 × 6.5 deg area at 114 cm from the observer with the yellow background (shown in grey in Fig. 1) extending over 17 × 13.5 deg. Figure 1 shows two spatial periods and one temporal period of the stimuli. Notice that the spatial duty-cycle of the direct- and reverse-phi components is 1:3; the stimulus may thus be looked at as consisting of bright and dark yellow vertical bars on an average luminance, yellow background. While the reverse-phi component (whose contrast is specified by a "1" in Fig. 1) requires that the displaced bars change polarity across frames, the direct-phi components (specified by a "2") may be built of either positive (brighter than the "background", as shown in Fig. 1) or negative (darker than the "background") polarity bars. All experimental conditions were run with both polarities.

The fundamental spatial and temporal frequencies of the two components were always identical and were varied in a range from 0.5 to 10 c/deg and from 2.5 to 15 Hz, respectively. 15 Hz is the maximum drift rate that can be obtained for these configurations with a 60 Hz video raster (i.e. 16.6 msec/frame). By necessity, it requires an unbalanced temporal duty-cycle ratio with zero OFF (spatially unmodulated) video frames. Lower modulation rates were obtained while keeping the temporal duty-cycle ratio at one, i.e. an equal number of ON and OFF frames (1/1, 2/2 and 3/3).

Procedure

The contrast of one of the two components (i.e. the direct- or reverse-phi) of the compound stimuli (configurations #1 and 2 in Fig. 1) was fixed, while the contrast of the second component was chosen randomly across trials from a preset pool of four or five contrasts (method of constant stimuli; contrasts were estimated in preliminary experiments so as to bracket the point of subjective equality (PSE), i.e. 50% "correct"; see below). Fixed- and variable-contrast components for each configuration were swapped across sessions. Fixed contrasts were set at 10% for all spatiotemporal conditions excepting those with spatial frequencies of 6.66 and 10 c/deg where they were set at 40%. This preserved the visibility of the fixed components about constant over the whole spatiotemporal range. Given equations (6) and (8), the S_{II}/S_I ratios should not depend on the particular "reference" contrast.

The observers' task was to specify the perceived direction (i.e. leftward versus rightward) of a given configuration. If the response coincided with the actual direction of the direct-phi component, the response was considered "correct". Datum points were obtained by means of a 2AFC procedure and were expressed as percentages "correct" (which could vary from 0 to 100%). Each session consisted in 200 or 250 trials depending on whether 4 or 5 contrasts were used (i.e. 50 trials per contrast). Each stimulus presentation consisted of eight "stimulus frames" (i.e. two temporal periods). Direction was randomized across trials. One session was defined by the stimulus configuration, the component whose contrast was fixed, the polarity of the direct-phi component and the spatiotemporal characteristics of stimulation. Each session was repeated at least twice so that final percentages "correct" were computed out of at least 100 trials per experimental point. For each condition, percentages "correct" as a function of contrast were fitted with Quick's psychometric function by means of Watson's (1979) algorithm with both α (the "threshold" or PSE at 50% "correct") and β (the slope) as free parameters. PSEs obtained with direct-phi components of positive and negative polarities were practically identical and were therefore averaged.

As a first step, configuration #1 was used under all spatiotemporal conditions. However, direction reversals (i.e. % "correct" $\leq$ 50%) could not be obtained for spatial and temporal frequencies lower than 2.5 c/deg and 7.5 Hz, respectively. In this range, a reverse-phi stimulus presented alone always yielded close to 100% "correct" responses, i.e. an absence of the reverse-phi effect. Conversely, configuration #2 could not elicit a perceived direction reversal outside this spatiotemporal range. Consequently, the final data were collected with the two configurations as shown in Table 1.

Two well-trained undergraduate students served as observers. One of them completed the experiments as part of her Master dissertation. The other was naive and was run only under conditions where the direct-phi component in both stimulus configurations was set at a

TABLE 1. Spatiotemporal conditions under which stimulus configurations #1 (unshaded) and #2 (shaded) were used. Digits refer to the fixed contrast of either one of the two stimulus components

Temporal frequency (Hz)	Spatial frequency (c/deg)					
	0.5	1.0	2.5	4.0	6.7	10.0
2.5	0.1	0.1	0.1	0.1	0.4	0.4
3.75	0.1	0.1	0.1	0.1	0.1	0.4
7.5	0.1	0.1	0.1	0.1	0.1	0.4
15.0	0.1	0.1	0.1	0.1	0.1	0.4

positive polarity. The vision of both observers was corrected to normal. Vision was binocular with natural pupils.

RESULTS

Figure 2 displays the S_{II}/S_I ratios for observers IB (A) and SJ (B) as computed from equations (6) and (8) depending on the specific stimulus configuration used (see Table 1). S_{II}/S_I ratios are shown as a function of spatial frequency with temporal frequency as a parameter. Symbols and straight lines are the actual data. The negative ratio (implying a negative sensitivity) obtained for observer SJ at 15 Hz is obviously due to measure error. Solid curves are power functions fitted to the data.

The general trend of the measured S_{II}/S_I ratios is obvious: they decrease with both spatial and temporal frequency. In other words, the sensitivity of the Fourier system, S_I, increases relatively to the sensitivity of the non-Fourier system, S_{II}, when either the spatial or the temporal frequency of the stimulus is increased. S_{II} is higher than S_I only for spatial and/or temporal frequencies below about 1 c/deg and 4 Hz, respectively (see Fig. 2 where the dashed horizontal line shows a S_{II}/S_I ratio of 1; also see Figs 4A and B). These observations are true

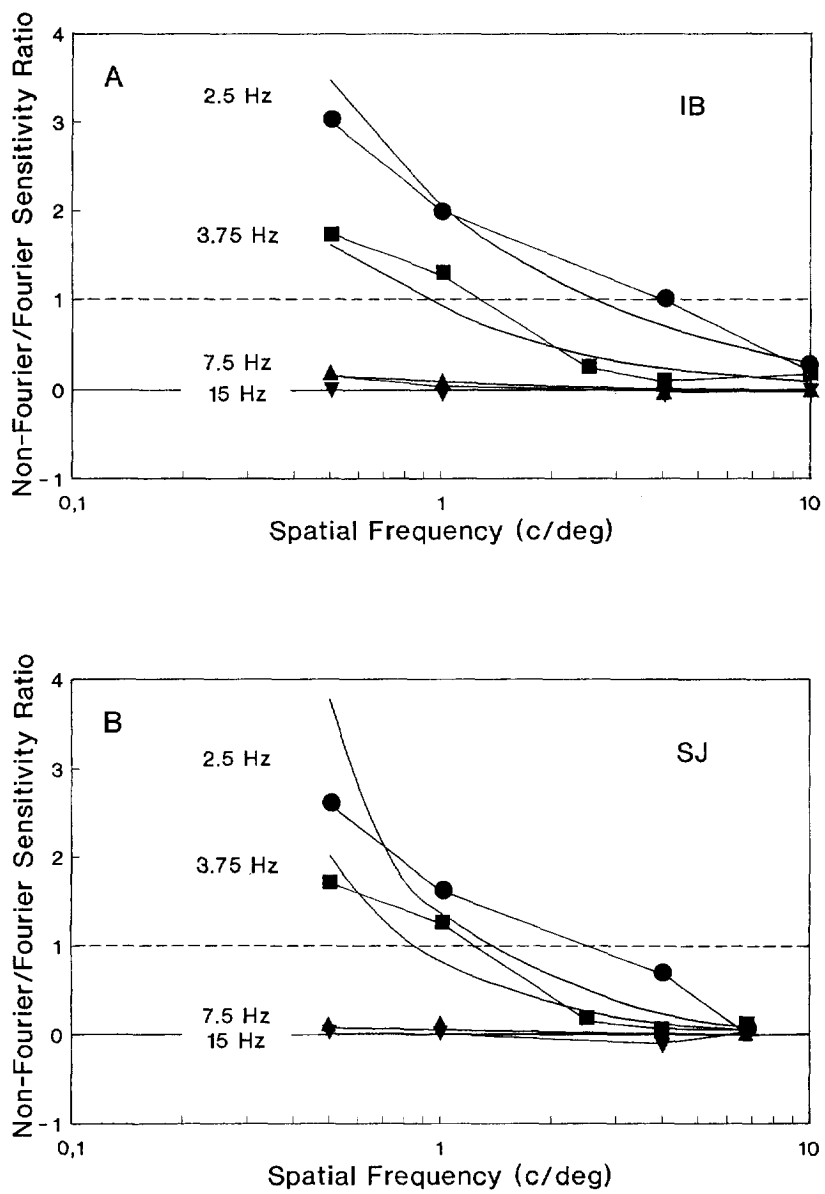

FIGURE 2. S_{II}/S_I ratios for two observers (A and B) as a function of spatial frequency with temporal frequency as a parameter. Symbols and straight lines show the empirical data (as derived from equations (6) and (8)). Bold curves are power regressions. The horizontal dashed line shows a S_{II}/S_I ratio of 1.

for both observers. The exponents of the adjusted power functions in Fig. 2 decrease from about −0.8, at 2.5 Hz to about −1, at 15 Hz, for both observers. The general trend of the data is better grasped in the three-dimensional display of Fig. 3 where S_{II}/S_I ratios are averaged across observers. The general and only conclusion that can be drawn from these data is that the non-Fourier system dominates visibility within a rather restricted region of the "window of visibility" characterised by low spatial and low temporal frequencies, while the Fourier system dominates visibility everywhere else. As discussed in the Rationale Section, the present experimental setup does not allow the independent specifications of S_I and S_{II}.

TENTATIVE SPECIFICATION OF S_I AND S_{II}

On the assumption that the Fourier and non-Fourier systems contribute independently to the classical spatiotemporal sensitivity surface (e.g. Robson, 1966; Kelly, 1979), one may specify their respective sensitivity surfaces so that (1) their ratios fit the empirical S_{II}/S_I ratios, R [equation (9)], and that (2) their probabilistic sum (Watson, 1979) fits the spatiotemporal sensitivity surface, S [equation (10)]:

$$S_{II}/S_I = R \tag{9}$$

$$(S_I^3 + S_{II}^3)^{1/3} = S. \tag{10}$$

The probability summation exponent in equation (10) was chosen to match the average exponent found in the literature (e.g. Watson, 1979; Gorea, 1986). The spatiotemporal sensitivity surface was specified by means of Kelly's (1979; see his equations (5)–(8), p. 1345) analytical expression:

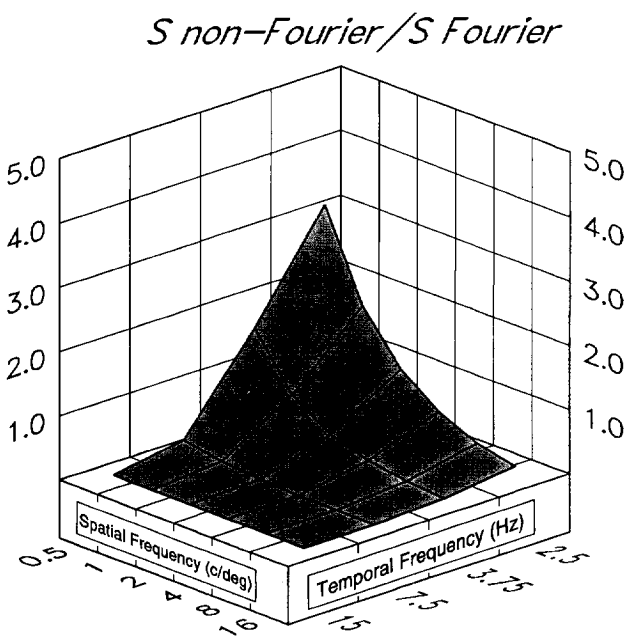

FIGURE 3. Three-dimensional representation of the mean S_{II}/S_I ratios as a function of both spatial and temporal frequency.

$$S(sf, tf) = [6.1 + k_1 |\log(tf/3sf)|^3] \times tf\alpha^2/s \exp[2\alpha(tf/sf + 2)/k_2], \tag{11}$$

with sf and tf standing for the spatial and temporal frequency, $\alpha = 2\pi$ and k_1 and k_2, two scale factors related to the peak frequency and to the peak sensitivity of the sensitivity surface. Kelly's best data fitting for the overall spatiotemporal surface was obtained with $k_1 = 7.3$ and $k_2 = 45.9$. Solving for equations (9) and (10) for each of the tested spatial and temporal frequency combinations enabled the specification of S_I and S_{II} under these conditions. The spatiotemporal sensitivity surfaces of the non-Fourier and Fourier systems (limited to the tested conditions) are shown in Figs 4A and B. Kelly's sensitivity surface obtained by means of equation (11) is shown for the same limited spatiotemporal range in Fig. 4C, and for a larger spatiotemporal range in Fig. 4D (note that the spatial and temporal frequency axes in Figs 4A, B and C are different from those in Fig. 4D).

Obviously, the spatiotemporal characterisation of the two motion systems provided here is questionable on many grounds and should not be regarded as definitive. Nonetheless, while awaiting for experimental techniques capable of providing a more direct characterisation, the spatiotemporal surfaces displayed in Figs 4A and B point to the following observations: (i) within the tested range, the non-Fourier system reaches its peak sensitivity (≈560) around 4 c/deg and 2.5 Hz or less. Its sensitivity drops drastically for spatial and temporal frequencies above 4 c/deg and 4 Hz. (ii) The peak sensitivity of the Fourier system (≈650) is reached somewhere between 4 and 8 c/deg and between 3 and 4 Hz. (iii) The two systems show a significant amount of spatiotemporal overlap. (iv) Kelly's peak sensitivity (≈1850) is reached around 4 c/deg and 0.5 Hz. Since Fig. 4B shows that the sensitivity of the Fourier system is quite low in this range, it should be assumed that the peak sensitivity of the non-Fourier system increases beyond the temporal frequency range used in the present experiments (Fig. 4A), i.e. for temporal frequencies below 2.5 Hz. Thus, the maximum sensitivity of the human observer appears to be due to the contribution of the non-Fourier system.

DISCUSSION

As already mentioned in the Rationale section, the present characterisation of the Fourier and non-Fourier systems is based on a simplified account of the underlying Reichardt-like processing units. The estimated S_{II}/S_I ratios might have been different had the front-end filtering properties of such units been more elaborated (see Chubb & Sperling, 1991). In particular, one may wish to consider the specific non-linearity characterizing the non-Fourier system and the space–time non-separability problem. Concerning the former, Chubb and Sperling (1989b, 1991) have already demonstrated that a half-wave rectification does a good job in accounting for the perception of a certain class of moving stimuli. However, only full-wave rectification can account for the

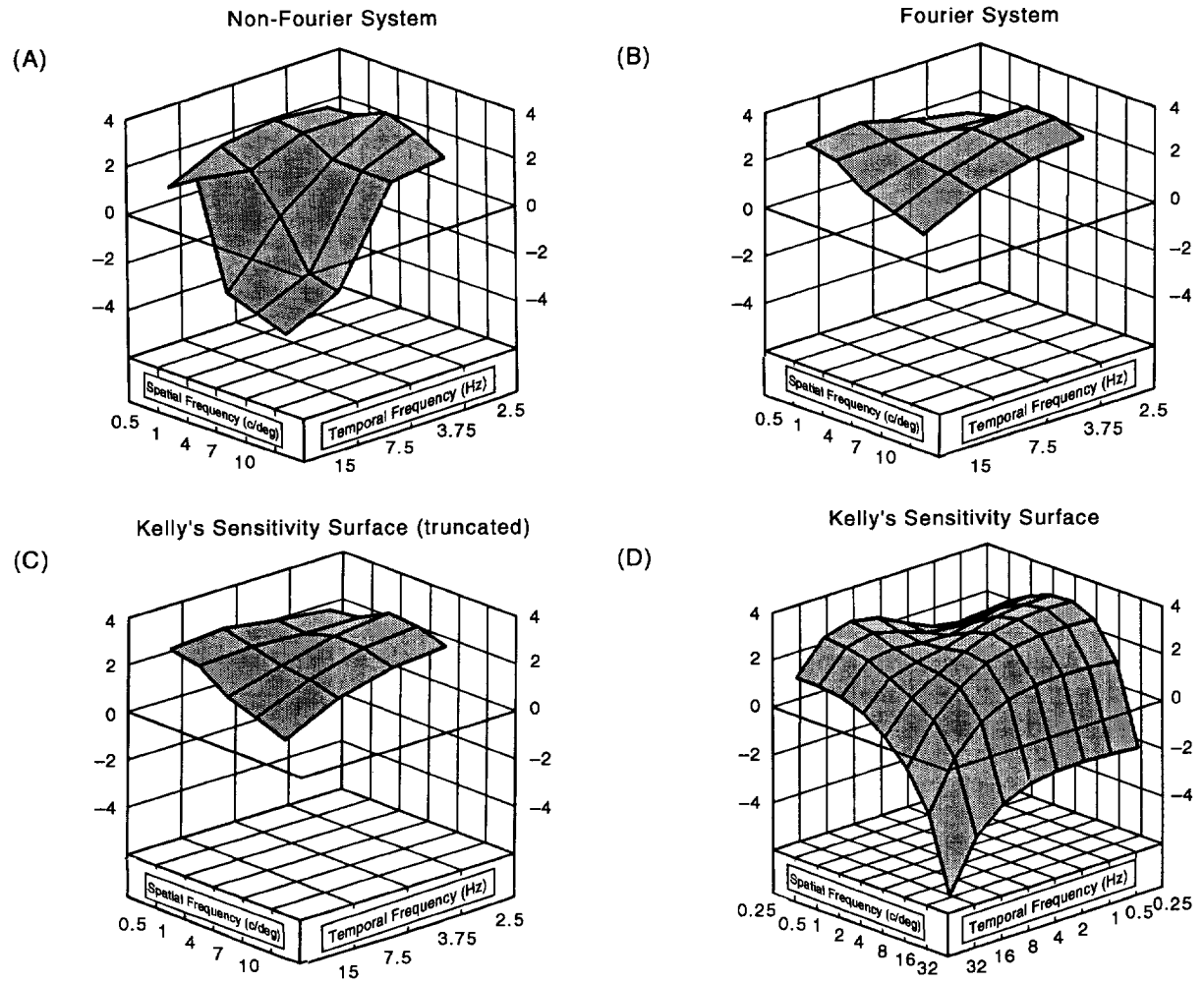

FIGURE 4. Sensitivities of the non-Fourier (A) and Fourier (B) systems as estimated given Kelly's (1979) spatiotemporal sensitivity surface (C and D). Note that the spatial and temporal frequency axes are the same for A, B and C and different for D. Only the latter are logarithmic. In C, Kelly's surface has been truncated to facilitate comparison with the estimated surfaces in A and B.

veridical perception (i.e. in the physical direction) of the reverse-phi stimuli used in this study.

The computations performed in this work roughly took into account the space–time non-separability of the visual system: they were performed with biphasic temporal impulse responses for the lowest two spatial frequencies (0.5 and 1 c/deg) and with monophasic ones for higher frequencies (e.g. Gorea & Tyler, 1986).* A progressive transition from biphasic to monophasic responses would have yielded slightly different sensitivity ratios. However, the spatiotemporal characteristics revealed in the present study are in good accord with those already specified in the literature for the short- and long-range motion systems (Braddick, 1974; see for a review Cavanagh & Mather, 1989), or alluded to for the Fourier and non-Fourier motion systems (see Sperling, 1989). It is therefore reasonable to assume that, while the present modelling simplifications yield only an approximate spatiotemporal characterisation of the two mechanisms, the present inferences are not drastically different from what they might have been had the modelling of these mechanisms been more elaborated.

Finally, the question may arise whether the very existence of a Fourier/non-Fourier dichotomy (used as a premise in the present experiments) is sufficiently validated in the literature. It is true, at least in principle, that a Reichardt-like unit with a front-end non-linearity presenting both odd- and even-symmetric terms could account for motion perception of both first- and second-order stimuli (Jonathan Victor, personal communication). There are at least two lines of evidence in the literature providing support to the Fourier/non-Fourier distinction.

The first type of evidence is based on the test of the *transition invariance* principle proposed by Werkhoven *et al.* (1993). The transition invariance principle states that if the strength of a homogeneous motion trajectory

*As already discussed in the Rationale section, the temporal filter underlying the processing of spatial frequencies higher than about 2 c/deg is low-pass, that is, its impulse response is monophasic. The sensitivity ratios estimated in the present study do still vary with spatial frequency above this limit (see Fig. 2). This variation cannot thus be attributed to a progressive change in the profile of the temporal front-end filter (see also previous footnote).

A–A (i.e. obtained by displacing element A across space and time) is adjusted to match the strength of a heterogeneous, A–B trajectory (i.e. obtained by displacing while swapping element A with element B), then it should also match the strength of the homogeneous trajectory B–B. If this is not the case, then A–A and B–B motions must be processed by different mechanisms. This logic has been applied since in different contexts both by Chubb *et al.* (personal communication) and by Papathomas, Gorea and Chubb (1994). The latter contribution clearly demonstrates the violation of transition invariance with stimuli where the A and B elements are luminance (Fourier) and contrast (non-Fourier) modulations.

The second line of evidence supporting the existence of at least two motion systems comes from studies where luminance and chromatic information were combined along the motion path. These studies demonstrated that color and luminance combine to yield motion perception at low, but not at medium-to-high temporal frequencies (Gorea *et al.*, 1993a, b). This observation cannot be accounted for by posing the existence of a unique motion system, whatever the type of non-linearity one might assume. Instead, these data point to the existence of an *unspecific* motion system, a system which discards stimulus qualia, and of a *specific* system which operates within a restricted domain (such as the luminance and chromatic domains) and on specific classes of primitives (such as spatial frequency, orientation, etc.). Another way to phrase this distinction is to say that the specific system *respects the similarity principle* (in the sensory domain), while the unspecific system does not respect this principle (Gorea *et al.*, 1993b). The specific system can therefore be represented as a battery of as many motion sensors as there are distinct filters. In contrast, the unspecific system can be regarded as a unique, low-pass filter combining all sources of stimulation. The temporal characteristics of these systems are very similar to those revealed in the present study with pure luminance stimuli. Insofar as full-wave rectification may be regarded as an operation whereby polarity information is discarded (by pooling signals from ON and OFF channels along the motion path), it may also be considered as a particular case of a more general "unspecificity" in motion processing. It is then tempting to assume that the Fourier/non-Fourier dichotomy is encompassed by the more general distinction between specific and unspecific motion mechanisms. Further experiments are needed to clarify this point.

REFERENCES

Adelson, E. H. & Bergen, J. R. (1985). Spatiotemporal energy models for the perception of motion. *Journal of the Optical Society of America A, 2*, 284–299.

Anstis, S. M. (1980). The perception of apparent motion. *Philosophical Transactions of the Royal Society, London, B290*, 153–168.

Anstis, S. M. & Mather, G. (1985). Effects of luminance and contrast on direction of ambiguous apparent motion. *Perception, 14*, 167–179.

Braddick, O. (1974). A short-range process in apparent motion. *Vision Research, 14*, 519–527.

Cavanagh, P. & Mather, G. (1989). Motion: The long and short of it. *Spatial Vision, 4*, 103–129.

Chubb, C. & Sperling, G. (1987). Drift-balanced stimuli: a general basis for studying non-Fourier motion perception. *Investigative Ophthalmology and Visual Science (Suppl.), 28*, 233.

Chubb, C. & Sperling, G. (1988a). Processing stages in non-Fourier motion perception. *Investigative Ophthalmology and Visual Science (Suppl.), 29*, 266.

Chubb, C. & Sperling, G. (1988b). Drift-balanced random stimuli: A general basis for studying non-Fourier motion perception. *Journal of the Optical Society of America A, 5*, 1986–2007.

Chubb, C. & Sperling, G. (1989a). Apparent motion derived from spatial texture. *Investigative Ophthalmology and Visual Science (Suppl.), 30*, 425.

Chubb, C. & Sperling, G. (1989b). Two motion perception mechanisms revealed by distance driven reversal of apparent motion. *Proceedings of the National Academy of Sciences U.S.A., 86*, 2985–2989.

Chubb, C. & Sperling, G. (1991). Texture quilts: Basic tools for studying motion-from-texture. *Journal of Mathematical Psychology, 35*, 411–442.

Chubb, C., McGowan, D., Sperling, G. & Werkhoven, P. (personal communication).

Gorea, A. (1986). Spatial integration characteristics in motion detection and direction identification. *Spatial Vision, 1*, 85–102.

Gorea, A., Papathomas, T. V. & Kovacs, I. (1993a). Two motion systems with common and separate pathways for color and luminance. *Proceedings of the National Academy of Sciences U.S.A., 90*, 11197–11201.

Gorea, A., Papathomas, T. V. & Kovacs, I. (1993b). Motion perception with spatiotemporally matched chromatic and achromatic information reveals a "slow" and a "fast" motion system. *Vision Research, 33*, 2515–2534.

Gorea, A. & Tyler, C. W. T. (1986). New look at Bloch's law for contrast. *Journal of the Optical Society of America A, 3*, 52–61.

Kelly, D. H. (1969). Flickering patterns and lateral inhibition. *Journal of the Optical Society of America, 59*, 1361–1370.

Kelly, D. H. (1979). Motion and vision. II. Stabilized spatio-temporal threshold surface. *Journal of the Optical Society of America, 69*, 1340–1349.

Papathomas, T. V., Gorea, A. & Chubb, C. (1994). One or multiple motion systems? *Perception, 23*, 61A.

Robson, J. G. (1966). Spatial and temporal contrast-sensitivity functions of the visual system. *Journal of the Optical Society of America, 56*, 1141–1142.

Sperling, G. (1989). Three stages and two systems of visual processing. *Spatial Vision, 4*, 183–207.

van Santen, J. P. H. & Sperling, G. (1984). Temporal covariance model of human motion perception. *Journal of the Optical Society of America A, 1*, 451–473.

van Santen, J. P. H. & Sperling, G. (1985). Elaborated Reichardt detectors. *Journal of the Optical Society of America A, 2*, 300–321.

Watson, A. B. (1979). Probability summation over time. *Vision Research, 19*, 515–522.

Watson, A. B. (1982). Derivation of the impulse response: Comments on the method of Roufs and Blommaert. *Vision Research, 22*, 1335–1337.

Werkhoven, P., Snippe, H. P. & Koenderink, J. J. (1990). Metrics for the strength of low-level motion perception. *Journal of Visual Communication and Image Representation, 1*, 176–188.

Werkhoven, P., Sperling, G. & Chubb, C. (1993). The dimensionality of texture-defined motion: A single channel theory. *Vision Research, 33*, 463–485.

Wilson, H. R., Ferrera, V. & Yo, C. (1992). A psychophysically motivated model of two-dimensional motion perception. *Visual Neuroscience, 9*, 79–97.

Acknowledgements—The final version of this manuscript is tributary to helpful discussions with Curtis Baker, Thomas V. Papathomas and Charlie Chubb, and to the insightful comments of Jonathan Victor, one of the two referees. This work was supported by grant #91-074 (DRET). Parts of this study were presented at the *16th European Conference on Visual Perception*, Edinburgh, Scotland, 25–29 August 1993.